SPATIOTEMPORAL ANALYSIS OF SATELLITE-BASED TRACE GASES CONCENTRATIONS IN PORT OF MANILA, PHILIPPINES

Laurelly Joyce Aporto*[1], Marie Antoinette Latunio[1], Roseanne Ramos[1], and Ayin Tamondong[1]
[1]Department of Geodetic Engineering, University of the Philippines Diliman
Email: laaporto1@up.edu.ph, mlatunio@up.edu.ph, rvramos@up.edu.ph, amtamondong@up.edu.ph

KEY WORDS: Air Quality, Port of Manila, Sentinel-5P Remote Sensing, Emerging Hotspot Analysis

ABSTRACT: The Port of Manila, located in the most highly urbanized city in the Philippines, is a major source of air pollutants. There is no ground monitoring station near this port, hence the lack of a reliable tool to assess whether air pollutant concentrations in its vicinity are within the safe levels. This study investigates the spatiotemporal variability of air pollutants, specifically nitrogen dioxide (NO_2) and sulfur dioxide (SO_2), in the Port of Manila, Philippines using remotely sensed Sentinel-5P TROPOMI observations. Tropospheric vertical column densities (VCDs) of SO_2 and NO_2 were analyzed using Emerging Hotspot Analysis (EHSA) in ArcGIS. Analytical parameters include the spatial neighbors set to 8, the neighborhood time step set to 1, and the global window set to Individual time step – set to ensure enough spatial context and temporal information for the analysis. The findings from the analysis revealed several patterns and trends within a 10-km vicinity of the study area. The analysis indicated a significant relationship between port activities and the occurrence of hotspots, particularly intensifying and persistent hotspots from 2019 to 2023. A decrease in hotspots is observed in 2020, which coincides with the period of community quarantines imposed in Metro Manila, Philippines during the COVID-19 pandemic. However, the analysis of SO_2 concentrations reveals no significant spatiotemporal patterns. This research provides insights into the spatiotemporal variability of air pollutants in the Port of Manila and results may be used by local authorities in developing a port monitoring system appropriate for the city.

1. INTRODUCTION

Air pollution is the largest known environmental health risk, causing around 7 million deaths every year globally (World Health Organization, 2016). In the Philippines, urban areas are continuously facing worsening air quality conditions. As much as 25% of the Filipino population is exposed to yearly average particulate matter concentrations that are at least five times higher than the WHO guidelines. In the first quarter of 2021, six air quality monitoring stations around Metro Manila that detect particulate matter pollutants reported 93 µg/Ncm (De Vera-Ruiz, 2021).

Air quality is of significant concern in areas where industrialization and urbanization are well-developed. In particular, port and coastal areas are common hotspots of air pollutants. The harmful emissions of ships used in international trades release massive amounts of pollutants into the air (Sinay, 2021). It is estimated that the shipping industry emits around 940 million tons of carbon dioxide every year, making up 2.5% of the total global carbon dioxide emissions (UK Research and Innovation, 2021).

Anthropogenic and natural sources of air pollution cause regular fluctuations in ambient air quality; hence, air quality monitoring technologies are continuously being developed to gain a more holistic understanding of air pollution. Today's air quality monitoring systems range from conventional reference-grade FRM/FEM monitors to mobile air quality sensors, stationary low-cost air quality sensors, satellite remote sensing monitoring technology, and alternative monitoring methods (Clarity, 2021). One of these alternative non-conventional methods to monitor air quality is the use of remote sensing to monitor air pollutant concentrations over large study areas.

Satellite remote sensing is one of the most recent advances in air quality monitoring technology because of its capability to cover a broad region in a single image and due to its temporal resolution. The multi-platform system and new algorithm in the processing chain for satellite remote sensing allow for faster and more accurate emission inventories over a given area. The Copernicus Sentinel-5 Precursor Tropospheric Monitoring Instrument (S5p/TROPOMI), created by the European Space Agency (ESA), currently provides the most significant real-time observations of air quality (Dutta, 2021).

In particular, the Philippines has a significant problem in its air quality monitoring systems and access to air pollution data. A recent environmental report revealed that inadequacies in access to data on air pollution and quality are increasing the risk of air pollution for vulnerable people in the Philippines (Chen et al., 2022). Only 45% of residents in the Philippines, for instance, reside within 25 kilometers of an air quality monitoring station, the majority of which are situated in Metro Manila. Stationary air quality monitoring stations in the country are also rarely updated regularly, making the data acquired insufficient and outdated (DENR-EMB, 2021).

With the alarming pollutant concentrations in the country, the need to develop proper air quality monitoring systems and technologies in the Philippines is crucial as air pollution monitoring works to protect the safety of the public from highly polluting facilities and corporations. Commonly, ground station equipment is utilized to monitor air quality in the Philippines; however, these instruments are big, expensive, heavy, and location dependent. Thus, the study proposes the utilization of remote sensing techniques and satellite image processing to analyze the spatiotemporal variations of air pollutant (nitrogen dioxide [NO_2] and sulfur dioxide [SO_2]) concentrations over a selected port area in the Philippines.

The primary objective of this study is to analyze the spatiotemporal variations of air pollutant concentrations over the highly industrialized Port of Manila, Philippines. Specifically, this study aims to utilize Sentinel-5P TROPOMI data in assessing Nitrogen Dioxide (NO_2) and Sulfur Dioxide (SO_2) concentrations over the Port of Manila Philippines. Moreover, the study aims to analyze the spatial and temporal trends and variations in air pollutant concentrations.

2. METHODOLOGY

2.1 Data Collection

Spatial data of nitrogen dioxide (NO_2) and sulfur dioxide (SO_2) were accessed from the Sentinel-5P TROPOMI instrument via the Google Earth Engine platform. These Level 3 products provided the tropospheric vertical column densities of the pollutants. The Google Earth Engine facilitated the acquisition of these datasets, which were provided at a spatial resolution of approximately 1x1° (equivalent to approximately 1.111 km). Monthly average data for NO_2 and SO_2 were extracted from the available datasets, covering the time period from July 2018 to March 2023 for NO_2 and December 2018 to March 2023 for SO_2.

2.2 Data Processing

2.2.1 Generation of Buffer Zone

Based on global annual approximations, approximately 70% of worldwide ship emissions occur within a 400 km distance from coastlines (Sorte et. al., 2020), thus requiring the analysis on the immediate vicinity of port areas. The value of 10 km was selected as the buffer radius.

Figure 1. Study area (left) and 10KM buffer zone, outlined in yellow

2.2.2 Space Time Cube Creation

To assess the spatial and temporal trends of air pollutant concentrations, a space-time cube was created for the years 2019-2022 for both NO_2 and SO_2 datasets. The *Create Space Time Cube* tool in ArcGIS requires a minimum of then (10) time slices in order to structure the data into 10 time-step intervals. Thus, study periods with less than ten (10) monthly raster data, specifically 2018 and 2023, were not included in the space-time cube creation. With ArcGis Pro, space-time statistics and visualizations can be applied to raster data using the Space Time Pattern Mining toolbox. The methods and parameters for the creation of the space time cube, adapted from Buie (2022), is shown in Figure 2. The outputs include netCDF space-time cubes for each pollutant for each year from 2019 to 2022.

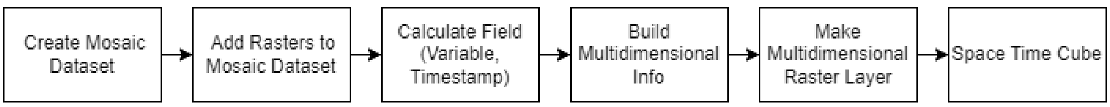

Figure 2. Space Time Cube creation in ArcGIS Pro 3.0 (Buie, 2022).

2.3 Emerging Hot Spot Analysis

2.3.1 Calculations

The spatiotemporal analysis of air pollutants was performed using the Emerging Hot Spot Analysis tool in ArcGIS Pro. Emerging Hot Spot Analysis (EHSA) is a technique categorized within the domain of exploratory spatial data analysis (ESDA) that combines two established methodologies. It integrates the conventional approach of hot spot analysis, employing the Getis-Ord Gi* statistic, with the classical time-series Mann-Kendall test for monotonic trends. The primary objective of EHSA is to assess the temporal dynamics of hot and cold spots. It facilitates the exploration of questions such as whether these spots are experiencing increasing intensity, undergoing cooling trends, or exhibiting stability over time (Parry, n.d.).

To accomplish this, EHSA calculates the Gi* statistic for each time period. The resulting series of Gi* values at each location is considered as a time-series dataset and subjected to the Mann-Kendall statistic to detect trends. The Getis-Ord Gi* statistic, as proposed by Ord and Getis (1995), was employed to identify the extent and intensity of spatial clustering.

The distribution of the Gi* statistic tends to follow a normal distribution when normality is observed in the variable. However, if the underlying distribution is non-normal, the test statistic also deviates from normality. In such scenarios, increasing the number of spatial units analyzed within the clusters can aid in approaching normality for the distribution of the Gi* statistic (Songchitruksa and Zeng, 2015). Under the assumption of normality, the Gi* statistic is typically standardized using its sample mean $\underline{X}$ and variance S^2:

$$G_i^* = \frac{\sum_{j=1}^{n} w_{i,j} x_j - \underline{X} \sum_{j=1}^{n} w_{i,j}}{S\sqrt{\frac{n\left[\sum_{j=1}^{n} w_{i,j}^2 - \left(\sum_{j=1}^{n} w_{i,j}\right)\right]^2}{n-1}}} \quad (1)$$

where x_j is the attribute value for feature j, $w_{i,j}$ is the spatial weight between feature i and j, n is equal to the total number of features and:

$$\underline{X} = \frac{\sum_{j=1}^{n} x_j}{n} \quad (2)$$

$$S = \sqrt{\frac{\sum_{j=1}^{n} x_j^2}{n} - \left(\underline{X}\right)^2} \quad (3)$$

The standardized Gi* is essentially a Z-score, allowing for its association with statistical significance. A Gi* value close to zero indicates a random distribution of the observed spatial events. Conversely, positive and negative Gi* statistics with high absolute values signify the presence of clusters with high- and low-valued events, respectively. Specifically, a negative Gi* suggests a tendency towards clusters of events characterized by short incident durations. In summary, if the calculated index values exceed a threshold associated with statistical significance, the location of a cluster is identified as a hotspot (Songchitruksa and Zeng, 2015).

Secondly, EHSA employs the Mann-Kendall trend test, initially introduced by Mann in 1945 and further developed by Kendall in 1975, to evaluate temporal trends observed throughout the time series data. The objective of the Mann-Kendall (MK) test (Mann, 1945; Kendall, 1975) is to conduct a statistical assessment of whether there exists a monotonic upward or downward trend in the variable of interest over time. A monotonic upward (or downward) trend implies a consistent increase (or decrease) of the variable throughout the time period, without necessarily adhering to a linear pattern.

The Mann-Kendall Trend test is a nonparametric test; meaning it does not rely on any specific distribution assumptions and is not influenced by outliers, making it advantageous for analyzing data variables that exhibit increasing or decreasing trends over time. However, the MK test is based on several underlying assumptions on the data to be analyzed. Firstly, in the absence of a trend, the measurements obtained over time should be independent and identically distributed. Independence implies that the observations are not correlated sequentially. Secondly, the observations collected over time should accurately represent the true conditions during the sampling periods. The methods employed for sample collection, handling, and measurement should yield unbiased and representative observations of the underlying populations across time. There is no strict requirement for the measurements to follow a normal distribution, nor is it necessary for the trend, if present, to be linear.

The MK test can accommodate missing values and values below the limits of detection (LD), but the presence of such occurrences can negatively impact the test's performance. Additionally, the assumption of independence necessitates that the time intervals between samples be sufficiently large to prevent correlation between measurements taken at different time points (Matzke et. al., 2014).

With a time series dataset comprising n observations of the variable of interest and for each pair of observations (x_j, x_k) where $j < k$, let $sgn(x_j - x_k)$ be an indicator function that takes on the values +1 for positive differences, -1 for negative differences, and 0 for tied differences. The MK test statistic is then calculated using the formula expressed in Equation 4.

$$
\begin{aligned}
Z_{MK} &= \frac{S-1}{\sqrt{VAR(S)}} if\ S > 0 \\
&= 0\ if\ S = 0 \\
&= \frac{S+1}{\sqrt{VAR(S)}} if\ S < 0
\end{aligned} \tag{4}
$$

where:

$$S = \sum_{k-1}^{n-1} \sum_{j-k+1}^{n} sgn(x_j - x_k) \tag{5}$$

and:

$$VAR(S) = \frac{1}{18}\left[n(n-1)(2n+5) - \sum_{p-1}^{g} t_p\,(t_p - 1)(2t_p + 5)\right] \tag{6}$$

where g is the number of tied groups and t_p is the number of observations in the pth group. A positive value of Z_{MK} suggests that the data exhibit a tendency to increase over time, while a negative value indicates a tendency towards decreasing values as time progresses.

2.3.2 Parameters

The Emerging Hot Spot Analysis tool involves setting the following parameters: conceptualization of spatial relationships, number of spatial neighbors, neighborhood time step, and global window. K nearest neighbor was used to conceptualize spatial relationships. The K-nearest neighbors (KNN) approach is particularly effective when ensuring a minimum number of neighbors for analysis becomes crucial. The KNN approach takes into account neighboring data points, regardless of their spatial distances, and incorporates their influence in the analysis. This enables the KNN approach to capture localized patterns and dependencies (ESRI, n.d.). Given that air quality data often exhibit spatial autocorrelation, meaning that neighboring locations tend to have similar values, the KNN method is suitable for this study.

The number of spatial neighbors was set to 8, the neighborhood time step was set to 1, and the global window was set to *Individual time step*. The *Number of spatial neighbors* and *Neighborhood Time Step* parameters determine the extent of each bin's neighborhood, which serves as the context for its analysis. KNN evaluates each pixel by evaluating the K number of neighbors (ESRI, n.d.). Given that the resolution of S5P datasets are approximately 1km x 1km, the hotspot analysis considers a neighborhood of 3km x 3km in the spatial clustering, as shown in Figure 3.

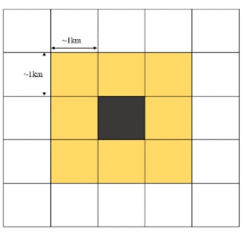

Figure 3. Spatial neighborhood for KNN analysis used in the study.

Furthermore, the temporal neighbors were considered using the time step parameter. Temporal neighbors are backward in time only and a neighborhood time step of 1 includes two time-step intervals — in the case of this study, two-month intervals. The global window, or what each bin is compared against to indicate statistical significance, was set to be the same as the neighborhood time step which is 1 or individual in order to examine how NO_2 and SO_2 concentrations are changing over time within the same spatial neighbors.

The selection of parameters in this study was centered around achieving a minimum number of neighbors and a minimum number of time steps in order to ensure sufficient spatial context and temporal information for the spatiotemporal analysis of air quality data.

2.3.3 EHSA Patterns

The outcomes obtained from the Getis Ord Gi* and Mann-Kendall statistics, pertaining to cluster and trend analyses, are subsequently employed to classify each bin. The Emerging Hot Spot Analysis tool assigns each bin to one of seventeen unique categories, encompassing a diverse range of scenarios. Each category represents a distinct configuration of spatiotemporal significance, allowing for a comprehensive characterization of the analyzed data (ESRI, 2014).

Table 1. Emerging Hotspot Analysis patterns in ArcGIS Pro 3.0 (ESRI, 2014).

Pattern Name	Definition
No Pattern Detected	Does not fall into any of the hot or cold spot patterns defined below.
New Hot Spot	A location that is a statistically significant hot spot for the final time step and has never been a statistically significant hot spot before.
Consecutive Hot Spot	A location with a single uninterrupted run of at least two statistically significant hot spot bins in the final time-step intervals. The location has never been a statistically significant hot spot prior to the final hot spot run and less than 90 percent of all bins are statistically significant hot spots.
Intensifying Hot Spot	A location that has been a statistically significant hot spot for 90 percent of the time-step intervals, including the final time step. In addition, the intensity of clustering of high counts in each time step is increasing overall and that increase is statistically significant.
Persistent Hot Spot	A location that has been a statistically significant hot spot for 90 percent of the time-step intervals with no discernible trend in the intensity of clustering over time.
Diminishing Hot Spot	A location that has been a statistically significant hot spot for 90 percent of the time-step intervals, including the final time step. In addition, the intensity of clustering in each time step is decreasing overall and that decrease is statistically significant.
Sporadic Hot Spot	A statistically significant hot spot for the final time-step interval with a history of also being an on-again and off-again hot spot. Less than 90 percent of the time-step intervals have been statistically significant hot spots and none of the time-step intervals have been statistically significant cold spots.
Oscillating Hot Spot	A statistically significant hot spot for the final time-step interval that has a history of also being a statistically significant cold spot during a prior time step. Less than 90 percent of the time-step intervals have been statistically significant hot spots.
Historical Hot Spot	The most recent time period is not hot, but at least 90 percent of the time-step intervals have been statistically significant hot spots.
New Cold Spot	A location that is a statistically significant cold spot for the final time step and has never been a statistically significant cold spot before.
Consecutive Cold Spot	A location with a single uninterrupted run of at least two statistically significant cold spot bins in the final time-step intervals. The location has never been a statistically significant cold spot prior to the final cold spot run and less than 90 percent of all bins are statistically significant cold spots.
Intensifying Cold Spot	A location that has been a statistically significant cold spot for 90 percent of the time-step intervals, including the final time step. In addition, the intensity of clustering of low counts in each time step is increasing overall and that increase is statistically significant.
Persistent Cold Spot	A location that has been a statistically significant cold spot for 90 percent of the time-step intervals with no discernible trend in the intensity of clustering of counts over time.
Diminishing Cold Spot	A location that has been a statistically significant cold spot for 90 percent of the time-step intervals, including the final time step. In addition, the intensity of clustering of low counts in each time step is decreasing overall and that decrease is statistically significant.
Sporadic Cold Spot	A statistically significant cold spot for the final time-step interval with a history of also being an on-again and off-again cold spot. Less than 90 percent of the time-step intervals have been statistically significant cold spots and none of the time-step intervals have been statistically significant hot spots.
Oscillating Cold Spot	A statistically significant cold spot for the final time-step interval that has a history of also being a statistically significant hot spot during a prior time step. Less than 90 percent of the time-step intervals have been statistically significant cold spots.

Historical Cold Spot	The most recent time period is not cold, but at least 90 percent of the time-step intervals have been statistically significant cold spots.

2.4 Temporal Analysis

In order to analyze the time periods with the most significant amounts of air pollutant concentrations within the study sites, box plots of NO_2 and SO_2 concentrations were utilized to analyze the temporal trends of various pollutant parameters by plotting the average vertical column density in monthly intervals. These plots provide a comprehensive summary of the dataset's distribution, including the minimum and maximum values, upper and lower quartiles, and the median. This approach allows for a detailed assessment of the temporal variations in air quality parameters.

3. RESULTS AND DISCUSSION

3.1 Emerging Hot Spot Analysis of NO_2 Concentrations

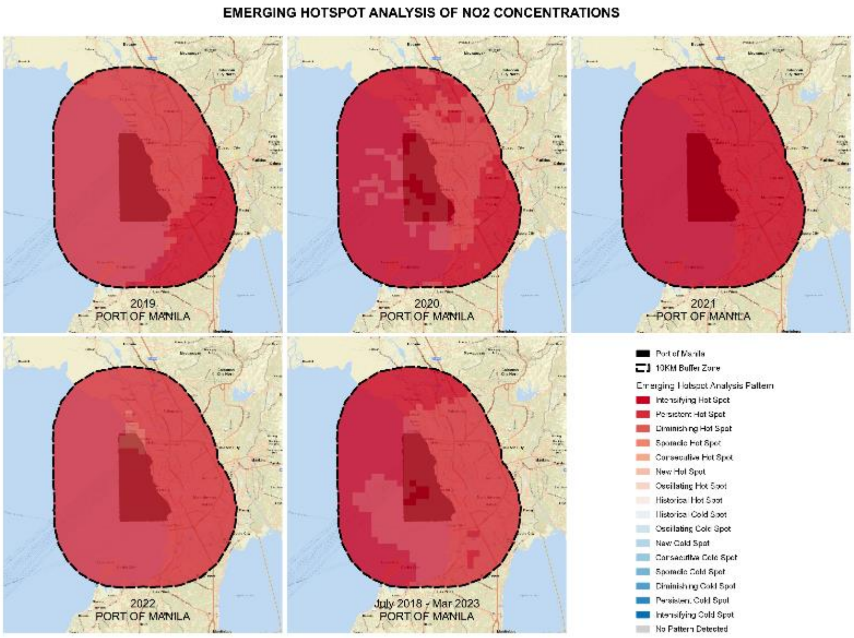

Figure 4. Emerging hotspot analysis of NO_2 concentrations in Port of Manila from 2019-2022

Emerging hotspot analysis of NO_2 tropospheric VCDs in the vicinity of Port of Manila highlights the regular occurrence of persistent and intensifying hotspots, coinciding with the high amount of activities in the port. Notably, the intensifying hotspots are clustered around land areas in Metro Manila while persistent hotspots are clustered around the port and coastal areas. Table 2 shows the percentages of the emerging hotspot analysis patterns of NO_2 in Port of Manila from 2019 to 2022 and their possible context and sources.

Table 2. Summary table of EHSA patterns of NO_2 concentrations in Port of Manila and their possible sources

Year	Pattern	Percentage (%)	Possible Source
2019	Persistent Hot Spot	79.24743	A 4.5 percent increase in container input of 5,315,500 twenty-foot equivalent units (TEUs) compared to the previous year of 2018 (Lloyd's List, 2021).
	Intensifying Hot Spot	20.75257	
2020	Intensifying Hot Spot	66.47662	A decrease of port activities and other related businesses due to the March 2020 COVID-19 community quarantine (Cigaral, 2020). It was reported later that year that the Port of Manila resumed normal operations after experiencing cargo congestion during the Luzon-wide lockdown (CNN, 2020).
	Persistent Hot Spot	33.52338	
2021	Intensifying Hot Spot	100	The Philippine Ports Authority reported in March of 2021 that cargo traffic in the Philippines is expected to rebound by 7% in 2021 after a 13.5% drop in 2020 due to pandemic-related restrictions. The decline was mainly observed in the

			ports of Manila, which handle 85% of the country's total cargo volume (Dela Cruz, 2021)
2022	Persistent Hot Spot	98.28962	The Philippine Ports Authority reported in 2022 that passenger volume in the Port of Manila more than doubled in the first half of the year, reflecting the easing of COVID-19 restrictions (Rosales, 2022).
	Diminishing Hot Spot	1.71038	

3.2 Emerging Hot Spot Analysis of SO_2 Concentrations

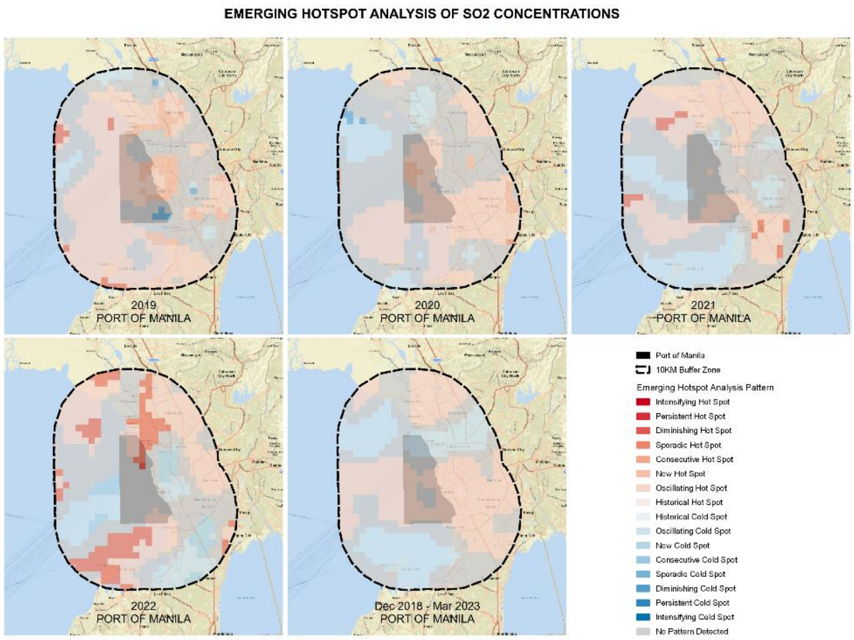

Figure 5. Emerging hotspot analysis of SO_2 concentrations in Port of Manila from 2019-2022

Emerging hotspot analysis on SO_2 tropospheric VCDs in the Port of Manila vicinity show that the overall most prevalent patterns are no pattern, oscillating hotspots, and oscillating coldspots. The 2019 emerging hotspot analysis resulted in an almost equivalent percentage of oscillating hotspots and no pattern detected while the 2020, 2021, and 2022 emerging hotspot analyses resulted in a majority of no pattern detected. The primary contributors of SO_2 in the Philippines are volcanic emissions (Canlas et. al., 2022). Despite this, it is worth noting that emerging hotspot analysis did not show any significant spatiotemporal patterns in SO_2 concentrations. Table 3 shows the percentages of the emerging hotspot analysis patterns of SO_2 in Port of Manila from 2019 to 2022 and their possible context and sources.

Table 3. Summary table of EHSA patterns of SO_2 concentrations in Port of Manila and their possible sources

Year	Pattern	Percentage (%)	Possible Source
2019	Oscillating Hot Spot	45.49601	The fluctuations in SO_2 levels as demonstrated by the prevalence of oscillating hotspots and cold spots can be attributed to the activity of the nearby Taal Volcano, which was declared Alert Level 1 on November 2019, Alert Level 4 then Alert Level 3 on January 2020, Alert Level 2 on March 2021, and Alert Level 3 on March 2022 (De Vera-Ruiz, 2019; De Vera-Ruiz, 2020; Arceo, 2021; ABS-CBN News, 2022).
	No Pattern Detected	40.59293	
	New Hot Spot	7.18358	
	Oscillating Cold Spot	3.87685	
	Sporadic Hot Spot	1.93843	
	Sporadic Cold Spot	0.91220	
2020	No Pattern Detected	51.53934	
	Oscillating Hot Spot	35.23375	
	Oscillating Cold Spot	9.69213	
	New Hot Spot	2.16648	
	Sporadic Cold Spot	0.57013	
	Sporadic Hot Spot	0.34208	
	Consecutive Hot Spot	0.22805	
	New Cold Spot	0.22805	
2021	No Pattern Detected	48.57469	

	Oscillating Hot Spot Oscillating Cold Spot Sporadic Hot Spot	32.95325 16.41961 2.05245	
2022	No Pattern Detected Oscillating Hot Spot Sporadic Hot Spot Oscillating Cold Spot New Cold Spot Diminishing Hot Spot	41.61916 27.13797 13.34094 11.63056 6.15735 0.11403	

3.3 Temporal Analysis

Table 4. Summary table of annual mean NO_2 concentrations in the study area

Year	Annual Mean NO_2 Concentrations within 10KM buffer zone (10^{-6} mol/m^2)
2019	98.929
2020	92.701
2021	95.216
2022	101.194

From the values presented in Table 4, percent change in the annual mean NO_2 concentrations in the study site, within their respective 10 KM buffer zone, was generated. There was a significant decline in the values of NO_2 from 2019 to 2020, quantitatively represented by the -6.30% percent change in the annual mean NO_2 concentrations. This is likely attributed to the COVID-19 lockdown during the aforementioned time period. Furthermore, there was an increase in the NO_2 concentrations in the area of Port of Manila, with a 6.28% percent change from 2021 to 2022. This can be attributed to the increased economic activity in the country as the strict COVID-19 lockdowns in the country were eased.

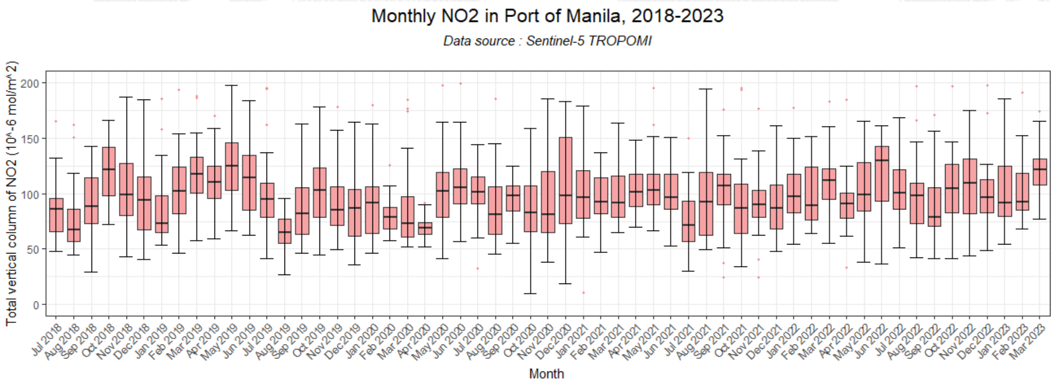

Figure 6. Box plots of monthly NO_2 concentrations in Port of Manila from 2018 - 2023.

Shown in Figure 6 is the variability of NO_2 concentrations in the Port of Manila from its monthly intervals from July 2018 to March 2023. Highest variability in pollutant concentration can be observed during June 2022 while lowest variability can be found during April 2020. Peak value can be observed during November 2021 while the lowest value, indicated as a significant outlier, can be seen during June 2022.

Table 5. Summary table of annual mean SO_2 concentrations in the study area

Year	Annual Mean SO_2 Concentrations within 10KM buffer zone (10^{-6} mol/m^2)
2019	0.138
2020	1.200
2021	9.085
2022	8.841

From the values presented in Table 5, percent change in the annual mean SO_2 concentrations in the study sites, within their respective 10 KM buffer zone, were generated. There was a significant increase in the values of SO_2 emissions in the study area from 2019 to 2020 likely due to the eruption of nearby Taal Volcano. Quantitatively, this increase is represented by the 772.00% percent change in the annual mean SO_2 concentrations in the Port of Manila. Furthermore, as the country seeks to spur economic activity, the strict COVID-19 lockdowns in the country were eased starting April 12, 2021. Thus, the further increase in the SO_2 concentrations in the study area.

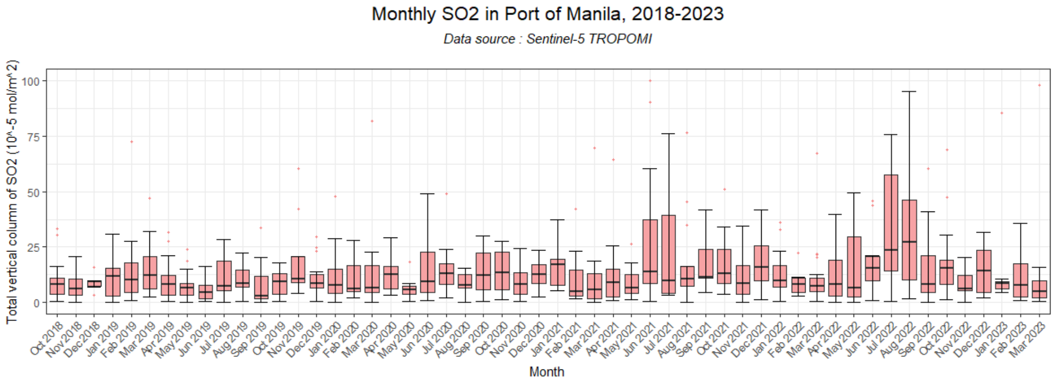

Figure 7. Box plots of monthly SO_2 concentrations in Port of Manila from 2018 - 2023.

The variability of SO_2 concentrations within the Port of Manila in monthly intervals from October 1, 2018 to March 31, 2023 is shown in Figure 7. Highest variability in pollutant concentration can be seen during months of July and August 2022 while the lowest variability can be found in November 2022. Peak value can be observed during January 2022 with significant outlier, while lowest values can be seen during April 2019.

4. CONCLUSIONS

The spatiotemporal variability of air pollutants NO_2 and SO_2 in Port of Manila, Philippines was studied through Emerging Hotspot Analysis of Sentinel-5P based tropospheric vertical column densities. The high spatio-temporal resolution measurements from Sentinel-5P were utilized to monitor the concentrations of trace gases. The findings from the Emerging Hotspot Analysis of NO_2 and SO_2 vertical column densities revealed several patterns and trends within the 10km vicinity of the study port area in the Philippines.

Spatial and temporal trends in air pollutant NO_2 and SO_2 concentrations were analyzed using the Emerging Hotspot Analysis tool. The study found a notable relationship between port activities and the occurrence of hotspots, particularly intensifying and persistent hotspots. The COVID-19 pandemic had an impact on the tropospheric vertical column densities, with a decrease in hotspots observed in 2020. Level of urbanization and the COVID-19 community quarantine proved to be the primary influencing factors in NO_2 concentrations. The declines in hotspots in these ports during the 2020 lockdowns are likely the result of reduced fuel combustion sources, such as decreased vehicle emissions and reduced output from power plants, which are significant contributors to NO_2 levels in urban areas. On the other hand, emerging hotspot analysis of SO_2 retrievals in Port of Manila revealed that there were no observable patterns. Analysis of annual mean concentrations proved to be consistent with the emerging hotspot analysis. Overall, The increase in mean NO_2 and SO_2 concentration values is directly related to the high amounts of intensifying and persistent hotspots in the port areas.

Future studies related to air quality monitoring in ports using remote sensing techniques can benefit from the following recommendations to enhance the analysis of air pollutant retrievals. Other trace gasses such as CO and CH_4 as well as other pollutants such as Particulate Matter (PM) can be explored to provide valuable insights into their sources and impacts. The inclusion of meteorological parameters such as wind speed and direction, rainfall, and land surface temperature (LST), which can significantly affect the dispersion and transportation of pollutants especially in port areas, can provide a more comprehensive understanding of the air quality dynamics. In addition, it can be beneficial to take into account all possible contributing factors, including the presence of neighboring establishments and population density. Finally, incorporating ground in situ data can be valuable for validation of remote sensing observations and contributing factors of air pollution in ports (i.e. cargo traffic, port and ship activities, volcanic emissions).

REFERENCES

ABS-CBN News, 2022. *Taal Volcano on Alert Level 3 indicating 'magmatic unrest'*.

Arceo, A., 2022. *Taal Volcano again emits high level of sulfur dioxide on August 7.* Rappler.

Buie, L., 2022. Investigate pollution patterns with space-time analysis. In *ESRI Documentation.*

Canlas, C. P., Sabuito, A. J., Veloria, A., & Perez, G. J., 2022. Time-Series Analysis of Air Quality in Major Cities in the Philippines During the COVID-19 Pandemic Through Sentinel-5. *Philippine Space Agency*.

Chen, Y.-J., Farrow, A., Wang, J., Chien, M.-J., Chiang, J., & Tan, L. K., 2022. *Different Air Under One Sky – The Inequity of Air Research*. Greenpeace India.

Cigaral, I. N., 2020. Cargoes, some holding food, stuck in Manila port amid lockdown. *Philstar Global*.

Clarity, 2021. *Air Quality Monitoring 2.0: How different types of air monitoring technologies are contributing to a more holistic understanding of air pollution*. Clarity Movement.

CNN, 2020. *Ports giant says Manila terminal operations are back to normal levels*.

De Vera-Ruiz, E., 2019. *Phivolcs Puts Taal Volcano Under Alert Level 1*. Manila Bulletin.

De Vera-Ruiz, E., 2020. *Alert Level 3 Raised as Taal Volcano Manifests Steam-Driven Explosion*. Manila Bulletin.

De Vera - Ruiz, E., 2021. *Air pollution levels in Metro Manila 59% lower in early hours of New Year's Day*. Manila Bulletin.

dela Cruz, R. C., 2021. PPA sees cargo traffic rebounding by 7% in 2021. *Philippine News Agency*.

DENR – Environmental Management Bureau, 2021. *Ambient Air Quality Monitoring Data*.

Dutta, V., Saroj Kumar & Dubey, D., 2021. Recent advances in satellite mapping of global air quality: evidences during COVID-19 pandemic. *Environmental Sustainability 2021 4:3*, *4*(3), 469–487.

ESRI, 2014. *How Emerging Hot Spot Analysis works*.

ESRI, n.d.. *Modeling spatial relationships—ArcGIS Pro | Documentation*.

Kendall, M.G., 1975. *Rank Correlation Methods*, 4th edition, Charles Griffin, London.

Lloyd's List, 2021. *41 Manila (Philippines)*.

Mann, H.B., 1945. Non-parametric tests against trend. *Econometrica*, 13:163-171.

Matzke, B. D., Newburn, L. L., Hathaway, J. E., Bramer, L. M., Wilson, J. E., Dowson, S. T., Sego, L. H., & Pulsipher, B. A., 2014. *Visual Sample Plan Version 7.0 User's Guide*.

Ord, J.K. and Getis, A., 1995. Local Spatial Autocorrelation Statistics: Distributional Issues and an Application. *Geographical Analysis*, 27(4).

Parry, J., n.d. *Emerging Hot Spot Analysis*.

Rosales, E. F., 2022. *PPA to decongest Manila ports*. Philstar Global.

Sinay, 2021. *How Do Ports Affect Air Quality? Air Quality Monitoring for Ports*.

Songchitruksa, P., & Zeng, X., 2010. Getis–Ord Spatial Statistics to Identify Hot Spots by Using Incident Management Data. *Transportation Research Record*, 2165(1), 42–51.

Sorte, S., Rodrigues, V., Borrego, C., & Monteiro, A., 2020. Impact of harbour activities on local air quality: A review. *Environmental Pollution*, *257*, 113542.

UK Research and Innovation, 2021. *Shipping industry reduces carbon emissions with space technology*. UKRI.

World Health Organization, 2016. *Ambient (Outdoor) Air Quality and Health*. Geneva.